

Half-solution to the two-body problem in General Relativity

Adrien Kuntz*

Aix Marseille Univ, Université de Toulon, CNRS, CPT, Marseille, France

(Dated: May 14, 2022)

We show that the introduction of two worldline parameters allows to drastically simplify computations in the effective field theory approach to the two-body problem in General Relativity, effectively removing half of the complexity in Feynman diagrams. These parameters obey a polynomial equation whose perturbative expansion recovers an infinite series of diagrams. Furthermore, we show that our equations define an effective two-body horizon for interacting black holes in General Relativity; in the circular orbit case, it corresponds to the smallest conceivable separation up to which the orbit can remain circular. We expect our results to simplify higher-order computations in the two-body problem, as well as to give insights on the nonperturbative properties of interacting binaries.

Gravitational waves (GW) from compact binaries [1, 2] provide exciting new challenges for our understanding of gravity in the strong-field regime. Waveform modeling require precise theoretical predictions on the two-body dynamics in General Relativity (GR) [3] for the LIGO/Virgo data analysis [4, 5], as well as for the future interferometers such as LISA [6] and Einstein Telescope [7]. The inspiral part is well described by the slow-motion, weak-field or post-Newtonian (PN) approximation [8], while for the last stages of the dynamics Numerical Relativity is needed [9]. More recently, Effective Field Theory (EFT) ideas from particle physics have been applied to the two-body problem [10, 11] in the framework of Non-Relativistic General Relativity (NRGR). The perturbative computations of the post-Newtonian approximation have been successfully translated in a series of Feynman diagrams. The current state-of-the-art computation in NRGR is at the 4PN level (i.e. v^8 beyond the Newtonian order where $v \ll 1$ is the typical velocity of the two bodies) [12–15]; this computation confirmed earlier results obtained in the PN formalism [16–23].

In NRGR as well as in the PN formalism, the binary constituents (considered nonspinning here for simplicity) are modeled as point-particles. The Feynman diagrams of the two point-particles involve graviton vertices connected by propagators. The vertices are of two types: the *bulk* nonlinearities originating from the Einstein-Hilbert action, and the *worldline* couplings coming from the matter action describing the two point-particles. In this Letter, we point out that the introduction of two worldline parameters - or einbeins [24] - allows to drastically simplify the worldline couplings, leaving an action containing only a *linear* coupling of the graviton to the source (similar parametrization was already used for the two-body problem in the context of modified gravity [25]). The number of Feynman diagrams needed to evaluate the action at each perturbative order is thus greatly reduced, so that the only computational obstacle in the two-body problem is entirely contained in the Einstein-Hilbert action.

Next, we investigate in more details the physical properties of the worldline parameters which we introduced.

In the case of circular orbits, these are known as the redshift variables [26, 27] as they represent the redshift of a photon emitted close to the point-particles and detected at large distance from the system. We find that these variables obey a fifth-order polynomial equation whose properties are examined in both the static and circular orbit case. We show that this equation does not admit solutions for close enough binaries, so that it allows to define an ‘effective two-body horizon’; more precisely, we find that for a critical separation no circular orbit can exist at all for the two-body problem. This is a two-body generalization of the well-known Innermost Circular Orbit (ICO) [28] of the Schwarzschild geometry. This result could shed light on nonperturbative properties of the two-body motion.

In the following we use units in which $\hbar = c = 1$, we define Planck’s mass by $M_{\text{P}}^2 = 1/(8\pi G)$ where G is Newton’s constant, and we use the mostly plus metric convention.

Integrating out gravity Let us begin by summarizing the NRGR approach to the two-body dynamics in GR [10, 11]. Along the way, we will introduce the worldline parameters. We take our action to be the one of GR, i.e

$$S = \frac{M_{\text{P}}^2}{2} \int d^4x \sqrt{-g} R + S_{m,1} + S_{m,2}, \quad (1)$$

where the matter action is constituted of two point-particles $\alpha = 1, 2$,

$$S_{m,\alpha} = -m_\alpha \int dt \sqrt{-g_{\mu\nu} v_\alpha^\mu v_\alpha^\nu}, \quad v_\alpha^\mu = \frac{dx_\alpha^\mu}{dt}. \quad (2)$$

In the NRGR formalism, the key quantity is the effective action formally defined as a path integral,

$$e^{iS_{\text{eff}}} = \int \mathcal{D}h_{\mu\nu} e^{iS}. \quad (3)$$

It is calculated with a Feynman expansion, by expanding the Ricci scalar and the point-particle action in powers of $h_{\mu\nu}$. The quadratic term defines the propagator of the gravitational field, while GR-nonlinearities give rise to an infinite series of vertices. The essential point of this

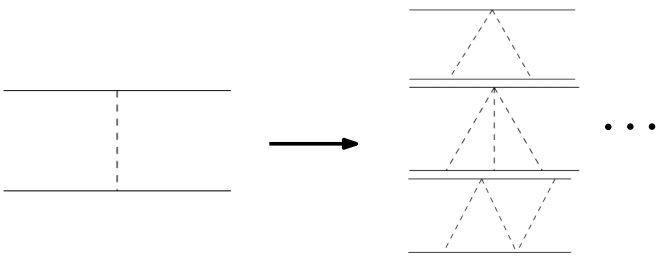


Figure 1. The only Feynman diagram arising from the linear coupling of Eq. 4, giving rise to an infinite series of diagrams involving nonlinear worldline couplings. The dotted line represents an insertion of the propagator, while the continuous lines represent point-particles treated as external sources.

Letter is that the nonlinearities associated to the point-particle action (we will refer to them as *worldline* nonlinearities) can be computed exactly, by introducing two auxiliary parameters. Let us rewrite each point-particle action as

$$S_{m,\alpha} = -\frac{m_\alpha}{2} \int dt \left[e_\alpha - \frac{g_{\mu\nu} v_\alpha^\mu v_\alpha^\nu}{e_\alpha} \right], \quad (4)$$

where the einbein e_α ensures reparametrization invariance of the action. Variation with respect to the einbein gives $e_\alpha = \sqrt{-g_{\mu\nu} v_\alpha^\mu v_\alpha^\nu}$ which yields back the original point-particle action 2. Instead, we will keep e_α undeter-

mined from now on and integrate out the gravitational field. The crucial improvement that this procedure yields is that the point-particle vertex is now *linear* in the gravitational field, allowing for an *exact* computation of the effective action.

Let us split $g_{\mu\nu} = \eta_{\mu\nu} + h_{\mu\nu}/M_{\text{P}}$. We add to the action the harmonic gauge-fixing term [10], so that our results will be expressed in harmonic coordinates. Expanding in $h_{\mu\nu}/M_{\text{P}}$, the total quadratic term in the action reads

$$S^{(2)} = -\frac{1}{8} \int d^4x \left[-\frac{1}{2} (\partial_\mu h_\alpha^\alpha)^2 + (\partial_\mu h_{\nu\rho})^2 \right], \quad (5)$$

which defines the propagator.

The theory defined by eqs. (5) and (4) is now a simple quadratic theory linearly coupled to two sources. We can thus obtain exactly the effective action. Of course this neglects the higher-order vertices in $h_{\mu\nu}$ arising from the expansion of the Einstein-Hilbert action and from the gauge-fixing term (we call them *bulk* nonlinearities in the following). These vertices are suppressed by 1PN order in the PN expansion, so that strictly speaking our computation will be of 0PN order. On the other hand our result should generalize the 1PM results [29], since the 1PM order consists in taking the full graviton propagator (5) with a linearized source term [30]. The couplings of the graviton to the point-particle give rise to *only* one Feynman diagram, represented in Figure 1. It is easily computed and gives an effective action

$$S_{\text{eff}} = \int dt \left[-\frac{m_1}{2} \left(e_1 + \frac{1 - v_1^2}{e_1} \right) + (1 \leftrightarrow 2) + \sum_{n \geq 0} \frac{(-1)^n}{(2n)!} \frac{d^{2n}}{dt_1^n dt_2^n} \left[\frac{Gm_1 m_2 \lambda(t_1, t_2)}{e_1(t_1) e_2(t_2)} |\mathbf{x}_1(t_1) - \mathbf{x}_2(t_2)|^{2n-1} \right]_{t_1=t_2=t} \right], \quad (6)$$

where λ is a combination of the two velocities,

$$\lambda = 1 + v_1^2 + v_2^2 - 4\mathbf{v}_1 \cdot \mathbf{v}_2 - v_1^2 v_2^2 + 2(\mathbf{v}_1 \cdot \mathbf{v}_2)^2, \quad (7)$$

where it is understood that \mathbf{v}_α should be evaluated at the corresponding time t_α in Eq. (6). Note that the last term of Eq. (6) is *not* a total derivative as it may seem at first glance. Also, let us highlight the fact that we have integrated out potential gravitons only, so that the Lagrangian (6) is conservative. In this article we do not consider the dissipative channels which are represented in the NRGR formalism as the emission of on-shell gravitons [11].

Post-Newtonian expansion We will now show how to recover a standard PN expansion from the Lagrangian (6). Let us first focus on the Lagrangian obtained from (6) by neglecting the retardation effects. This means that we replace the sum by its $n = 0$ term. To get the effective two-body dynamics from this Lagrangian, one should integrate out the two auxiliary parameters. This

imply a fifth-order equation for e.g e_1 ,

$$(e_1^2 - 1 + v_1^2)^2 \left(e_1(1 - v_2^2) - \frac{2\lambda Gm_1}{r} \right) - \frac{4\lambda^2 G^2 m_2^2 e_1}{r^2} = 0, \quad (8)$$

with labels interchanged for e_2 . By applying the post-Newtonian scaling $1/r = \mathcal{O}(v^2) \ll 1$ it is easy to perturbatively solve this equation. There are four branches of solutions and we select the one whose PN expansion is consistent. At the 1PN order, we find the Lagrangian

$$L_{1\text{PN}} = \frac{1}{8} \left(m_1 v_1^4 + m_2 v_2^4 + 4 \frac{Gm_1 m_2}{r} (3v_1^2 + 3v_2^2 - 8\mathbf{v}_1 \cdot \mathbf{v}_2) + \frac{4G^2 m_1 m_2 (m_1 + m_2)}{r^2} \right). \quad (9)$$

This should correspond to the 1PN or Einstein-Infeld-

Hoffmann Lagrangian [31]. However, recall that we do not yet consider *bulk* nonlinearities, as well as propagators corrections coming from retardation effects. This means that our expression should only recover diagrams 4b, 4c and 5b of Ref. [10], and it is indeed the case. It is remarkable that by a single linear diagram one can get directly the diagrams with nonlinear worldline fields insertions such as diagram 5b of Ref. [10].

Going further, it is easy to check that when including retardation effects the full 1PN Lagrangian is recovered up to the only diagram with a cubic graviton vertex given by Figure 5b in Ref. [10]. We have also verified that we correctly obtain the 2PN diagrams corresponding to this resummation. [32].

Finite-size effects A great improvement of our approach compared to standard NRGR is that finite-size effect have a more direct graphical interpretation : they are the only non-minimal couplings to the point-particles worldlines. Following [11], we can model finite-size effects at lowest order by adding a term in the action

$$\frac{C_E}{M_{\text{P}}^2} \int dt (\partial_i \partial_j h_{00})^2, \quad (10)$$

where the coefficient C_E is related to Love numbers with a scaling $C_E \sim r_s^5/G$ with r_s the size of the source. We choose here to treat these kind of operators perturbatively, while still staying nonperturbative in the lowest-order point-particle coupling (2). Hence a simple computation gives the lowest-order contribution of finite-size effects to the effective Lagrangian (6) :

$$L_{\text{finite-size}} = 24i \frac{G^2 C_{E,1} m_2^2}{e_2^2 r^6} + (1 \leftrightarrow 2). \quad (11)$$

Static potential Having confidently established the perturbative validity of our Lagrangian (6), we will now analyze in more details the non-perturbative effects it implies. By non-perturbative we mean that we do not resort to any post-Newtonian expansion beyond the first approximation of ignoring bulk nonlinearities. This approach is similar in spirit to the post-Minkowskian expansion [29, 33–38]. Of course, there is no physically conceivable situation where the bulk nonlinearities would be subdominant while not being in a post-Newtonian approximation scheme. However, our results will be in some sense 'more exact' than the post-Newtonian ones since we include an infinite number of PN terms. We will see that we will be able to define an 'effective two-body horizon', a quantity whose very existence cannot be recasted in the standard post-Newtonian formalism.

To get some insight, we will begin by analyzing the static situation. This means that we will set $v_1 = v_2 = 0$ in all our preceding formulas. Then e_1, e_2 obey the quintic equation $f_\alpha(e_\alpha, r) = 0$ where

$$f_1(e_1, r) \equiv (e_1^2 - 1)^2 \left(e_1 - \frac{2Gm_1}{r} \right) - \frac{4G^2 m_2^2 e_1}{r^2}, \quad (12)$$

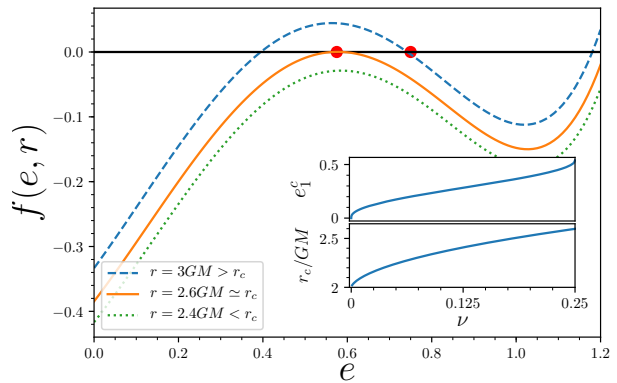


Figure 2. *Main plot*: Polynomial equation (12) in the equal-mass case $m_1 = m_2 = M/2$, for different values of r . The red dot represents the solution with the correct post-Newtonian behavior for $r \rightarrow \infty$. For r smaller than the critical radius r_c this solution becomes complex-valued. *Subplot*: Critical radius in units of GM and critical parameter e_1^c , as a function of the symmetric mass ratio $\nu = m_1 m_2 / M^2$. It is assumed that $m_1 < m_2$, so that in the test-mass limit $m_1 \rightarrow 0$, $r_c = 2GM = 2Gm_2$ and $e_1^c = 0$; in the equal-mass case, $r_c = 3\sqrt{3}GM/2 \approx 2.6GM$ and $e_1^c = 1/\sqrt{3} \approx 0.58$

with labels interchanged for e_2 .

The polynomial equation (12) has five roots and only one has the correct post-Newtonian expansion. In Figure 2 we have plotted the quintic equation (12) in the equal-mass case as a function of e_1 and for different values of r . It appears that for a certain critical value of the radius r_c , the real root $e_1(r)$ with the correct post-Newtonian behavior cease to exist. This critical radius is defined as the point where

$$f_1(e_1, r) = \frac{\partial f_1}{\partial e_1} = 0, \quad (13)$$

and is also plotted as a function of the symmetric mass ratio $\nu = m_1 m_2 / M^2$ (where $M = m_1 + m_2$) in Figure 2. Note that due to the symmetry of the equations, the critical radius is the same if one instead considers the polynomial equation on e_2 .

To get an understanding of the phenomenon at play, let us consider the test-mass ratio $m_1 \rightarrow 0$. In this case the critical radius becomes $r = 2Gm_2$. But we also know the exact solution for e_1 from the original point-particle action (4) : it is $e_1^2 = -\bar{g}_{00}$ where $\bar{g}_{\mu\nu}$ is the Schwarzschild metric in harmonic coordinates,

$$\bar{g}_{00} = -\frac{r - Gm_2}{r + Gm_2}. \quad (14)$$

More precisely, since we are considering a one-graviton exchange in the Lagrangian (6) we should rather take the linearized Schwarzschild metric so that $e_1^2 \approx 1 - 2Gm_2/r$. It is then clear that in this case the critical radius corresponds to the point-particle becoming lightlike $e_1 = 0$,

i.e the critical radius is reached when the point-particle is on the horizon of the massive particle m_2 . In this sense, our equations define an effective horizon for two interacting point-particles : for $r < r_c$, our static assumption is necessarily invalid since there are no solution to the equations, i.e the two particles are forced to move. We will translate this statement in a measurable gauge-invariant quantity in the following.

Of course, the true horizon of the Schwarzschild metric in harmonic coordinates is situated at $r = Gm_2$ and not at $r = 2Gm_2$. We expect that taking into account cubic and higher vertices would give a more accurate estimate of the location of the horizon. This is indeed the case when approximating the rational fraction (14) by polynomials of increasing degree in order to find its zero.

It is interesting to note that the disappearance of a solution of the quintic equation (12) is an intrinsically non-perturbative phenomenon. Indeed, if one tried to solve the quintic equation for e_1 (12) perturbatively as before, one would get e.g

$$e_1 = 1 - \frac{Gm_2}{r} - \frac{G^2m_2(m_2 + 2m_1)}{2r^2} + \mathcal{O}\left(\frac{1}{r^3}\right), \quad (15)$$

and this solution exists for all r . Likewise, one could solve equation (12) perturbatively in the mass ratio m_1/m_2 to get

$$e_1 = \sqrt{1 - \frac{2Gm_2}{r}} - \frac{G^2m_1m_2}{r(r - 2Gm_2)} + \mathcal{O}(m_1^2). \quad (16)$$

The point is that, as the lowest-order solution presents a singular behavior only at $r = 2Gm_2$, the same will be true of any perturbative order beyond the leading one, and so the solution for e_1 can never cease to exist for any r greater than $2Gm_2$ contrary to the behavior identified in Figure 2.

Another feature of the critical point is the characteristic behavior of e near to this point. One can define a 'critical exponent' γ by the scaling $e_1 - e_1^c \propto (r - r_c)^\gamma$ close to the critical point, with $\gamma = 1/2$. This is because the vanishing of the derivative of the polynomial equation $\partial f_1/\partial e_1 = 0$ at the critical point imposes that for e_1 close to e_1^c and r close to r_c ,

$$0 = f_1(e_1, r) \simeq (r - r_c) \frac{\partial f_1}{\partial r} + \frac{1}{2}(e_1 - e_1^c)^2 \frac{\partial^2 f_1}{\partial e_1^2}, \quad (17)$$

such that $e_1 - e_1^c \propto (r - r_c)^{1/2}$. This generalizes to any mass ratio the well-known behavior in the test-mass limit obtained from the definition of the einbeins, Eq. (4).

Circular orbits The preceding qualitative analysis is gauge-dependent and as such does not provide any physically measurable quantity. We now make the assumption that the two bodies follow an exactly circular orbit of frequency ω (we recall that we concentrate on the conservative dynamics). In this setting, a physical interpretation

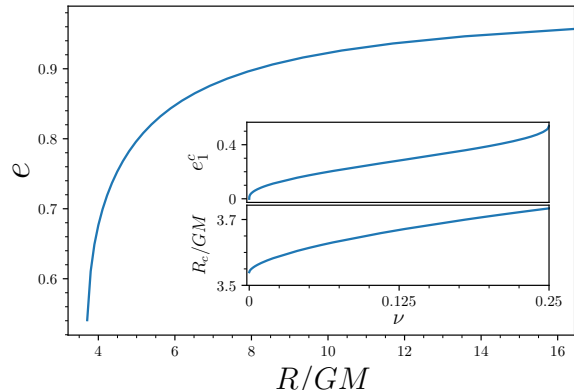


Figure 3. *Main plot*: Redshift function $e_1 = e_2 = e$ in the equal-mass case $m_1 = m_2$, plotted as a function of the gauge-invariant distance (18). The derivative of e at the critical radius is infinite. *Subplot*: Critical redshift e_1^c and radius R_c for different symmetric mass ratios ν . In the test-mass limit, $R_c \simeq 3.54GM$ and $e_1^c = 0$; in the equal-mass case, $R_c \simeq 3.73GM$ and $e_1^c \simeq 0.54$.

of the einbeins e_1, e_2 has been given by Detweiler [26]. Namely, these are the redshift of photons emitted near to the point-particles and detected by an observer situated far from the system on its axis of rotation, and as such are gauge invariant within the physically reasonable class of gauges defined in [27].

By rewriting the infinite sum in Eq. (6) as a dependence on retarded and advanced times, it is possible to solve for the equations of motion associated to this action. This derivation will be presented elsewhere [39]. The polynomial equation on e_α (8) now becomes a relation between the redshift variables and the frequency ω . We introduce the gauge-invariant distance

$$R = \left(\frac{GM}{\omega^2}\right)^{1/3}, \quad (18)$$

where $M = m_1 + m_2$, and plot the critical distance and redshift parameter (defined as the point where both the polynomial equation and its frequency derivative vanish) for different mass ratios in Figure 3.

Once again, the test-mass limit sheds light on the physical origin of the critical radius. It is well-known that the Schwarzschild geometry possess a last circular orbit at $R = 3GM$, under which no circular orbits (even unstable) can exist at all. This locus corresponds to the four-velocity v^μ of the point-particle becoming lightlike thus justifying its name of 'light-ring'. Our polynomial equation thus provides a generalization of this feature to the comparable-mass case : no circular orbit can exist at all beyond the critical radius. Moreover, for two particles approaching the critical point an observer would see an abrupt change in the redshift parameters. This is due to the critical behavior observed previously : at the

critical point (e_c, ω_c) , both the polynomial equation on e_α and its derivative vanishes, so that one has the scaling $e - e_c \propto (\omega - \omega_c)^{1/2}$ and the derivative of e_α at the critical point is infinite. This is illustrated in Figure 3.

Finally, note that the value of the critical radius in the test-mass limit $\nu \rightarrow 0$ is not the correct Schwarzschild result since our Lagrangian corresponds to a single graviton exchange. Indeed, our results in the test-mass limit can once again be recovered by considering the linearized Schwarzschild metric in harmonic coordinates,

$$ds^2 = - \left(1 - \frac{2GM}{r} \right) dt^2 + \left(1 + \frac{2GM}{r} \right) d\mathbf{x}^2. \quad (19)$$

In this test-mass limit, the critical point (determined by the equation $g_{\mu\nu}v^\mu v^\nu = 0$) is

$$R_c \simeq 3.54GM. \quad (20)$$

Thus our approximation overestimates the critical radius $R_c = 3GM$ in the test-mass limit ; this could be improved by taking into account higher-order nonlinear vertices in the Einstein-Hilbert action.

Conclusion In this Letter, we have shown that the introduction of two einbeins allows for a drastic simplification of the Feynman rules of NRGR ; diagrams of increasing complexity are simply recovered from the expansion of a polynomial equation. We thus expect our result to be particularly relevant for the computation of higher order PN dynamics.

Furthermore, the polynomial equations obeyed by the redshift variables allows to define an horizon for two interacting point-particles in GR. For circular orbits, the standard PN solution for the worldline parameters becomes complex-valued for small enough separations so that no circular orbit can exist at all beyond this critical distance. Taking into account cubic and higher-order vertices would give a more precise estimate of this minimal separation. More generally, the disappearance of PN solutions for close enough binaries points towards an inadequacy of the PN parameterization in this strong-field regime.

There are multiple avenues for extending and improving our results. Apart from the inclusion of higher PM orders [34], it would also be interesting to explore the synergies of our resummation with the Effective One-Body (EOB) [40] formalism. Indeed, while the EOB philosophy is to recast the two-body motion as the one of a point-particle in an effective metric, our resummation is somewhat two-body in essence : worldline nonlinearities do not contribute to the field of an isolated object, so that the Feynman diagrams included in our resummation contain only genuine two-body effects. On the other hand, our treatment misses the one-body dynamics (which is fully contained in the bulk nonlinearities), so that an EOB approach would be complementary.

Acknowledgments: I would like to thank Filippo Vernizzi, Vitor Cardoso, Scott Melville, Massimiliano

Maria Riva, Ira Rothstein and especially Federico Piazza for discussions and comments. This article is partly based upon work from COST Action GWVerse CA16104, supported by COST (European Cooperation in Science and Technology).

* kuntz@cpt.univ-mrs.fr

- [1] B. Abbott, R. Abbott, T. Abbott, F. Acernese, K. Ackley, C. Adams, T. Adams, P. Addesso, R. Adhikari, V. Adya, and et al., *Physical Review Letters* **119** (2017), 10.1103/physrevlett.119.161101.
- [2] B. P. Abbott *et al.* (LIGO Scientific, Virgo), *Phys. Rev. Lett.* **116**, 061102 (2016), arXiv:1602.03837 [gr-qc].
- [3] L. Lindblom, B. J. Owen, and D. A. Brown, *Physical Review D* **78** (2008), 10.1103/physrevd.78.124020.
- [4] J. Aasi, B. P. Abbott, R. Abbott, T. Abbott, M. R. Abernathy, K. Ackley, C. Adams, T. Adams, P. Addesso, and et al., *Classical and Quantum Gravity* **32**, 074001 (2015).
- [5] F. Acernese, M. Agathos, K. Agatsuma, D. Aisa, N. Allemandou, A. Allocca, J. Amarni, P. Astone, G. Balestri, G. Ballardín, and et al., *Classical and Quantum Gravity* **32**, 024001 (2014).
- [6] P. Amaro-Seoane, H. Audley, S. Babak, J. Baker, E. Barausse, P. Bender, E. Berti, P. Binetruy, M. Born, and D. B. et al., “Laser interferometer space antenna,” (2017), arXiv:1702.00786 [astro-ph.IM].
- [7] B. Sathyaprakash, M. Abernathy, F. Acernese, P. Ajith, B. Allen, P. Amaro-Seoane, N. Andersson, S. Aoudia, K. Arun, P. Astone, and et al., *Classical and Quantum Gravity* **29**, 124013 (2012).
- [8] L. Blanchet, *Living Rev. Rel.* **17**, 2 (2014), arXiv:1310.1528 [gr-qc].
- [9] P. Grandclément and J. Novak, *Living Reviews in Relativity* **12**, 1 (2009), arXiv:0706.2286 [gr-qc].
- [10] W. D. Goldberger and I. Z. Rothstein, *Physical Review D* **73** (2006), 10.1103/PhysRevD.73.104029, arXiv: hep-th/0409156.
- [11] R. A. Porto, *Physics Reports* **633**, 1 (2016), arXiv: 1601.04914.
- [12] S. Foffa and R. Sturani, *Physical Review D* **87** (2013), 10.1103/physrevd.87.064011.
- [13] S. Foffa, P. Mastrolia, R. Sturani, and C. Sturm, *Physical Review D* **95** (2017), 10.1103/physrevd.95.104009.
- [14] S. Foffa and R. Sturani, *Phys. Rev. D* **100**, 024047 (2019), arXiv:1903.05113 [gr-qc].
- [15] S. Foffa, R. A. Porto, I. Rothstein, and R. Sturani, *Phys. Rev. D* **100**, 024048 (2019), arXiv:1903.05118 [gr-qc].
- [16] T. Damour, P. Jaranowski, and G. Schäfer, *Physical Review D* **89** (2014), 10.1103/physrevd.89.064058.
- [17] T. Damour, P. Jaranowski, and G. Schäfer, *Physical Review D* **91** (2015), 10.1103/physrevd.91.084024.
- [18] T. Damour, P. Jaranowski, and G. Schäfer, *Physical Review D* **93** (2016), 10.1103/physrevd.93.084014.
- [19] L. Bernard, L. Blanchet, A. Bohé, G. Faye, and S. Marsat, *Physical Review D* **93** (2016), 10.1103/physrevd.93.084037.
- [20] L. Bernard, L. Blanchet, A. Bohé, G. Faye, and S. Marsat, *Physical Review D* **95** (2017), 10.1103/physrevd.95.044026.
- [21] L. Bernard, L. Blanchet, A. Bohé, G. Faye, and

- S. Marsat, Physical Review D **96** (2017), 10.1103/physrevd.96.104043.
- [22] T. Marchand, L. Bernard, L. Blanchet, and G. Faye, Physical Review D **97** (2018), 10.1103/physrevd.97.044023.
- [23] L. Bernard, L. Blanchet, G. Faye, and T. Marchand, Physical Review D **97** (2018), 10.1103/physrevd.97.044037.
- [24] D. Tong, “Lectures on string theory,” (2009), arXiv:0908.0333 [hep-th].
- [25] A.-C. Davis and S. Melville, arXiv e-prints , arXiv:1910.08831 (2019), arXiv:1910.08831 [gr-qc].
- [26] S. L. Detweiler, Phys. Rev. **D77**, 124026 (2008), arXiv:0804.3529 [gr-qc].
- [27] L. Blanchet, S. Detweiler, A. Le Tiec, and B. F. Whiting, *Mass and motion in general relativity. Proceedings, School on Mass, Orleans, France, June 23-25, 2008*, Fundam. Theor. Phys. **162**, 415 (2011), [415(2010)], arXiv:1007.2614 [gr-qc].
- [28] Defined as the smallest possible circular orbit; not to be confused with the Innermost *stable* Circular Orbit or ISCO.
- [29] C. Cheung, I. Z. Rothstein, and M. P. Solon, Phys. Rev. Lett. **121**, 251101 (2018), arXiv:1808.02489 [hep-th].
- [30] S. Foffa, Phys. Rev. **D89**, 024019 (2014), arXiv:1309.3956 [gr-qc].
- [31] A. Einstein, L. Infeld, and B. Hoffmann, The Annals of Mathematics **39**, 65 (1938).
- [32] The 2PN conservative Lagrangian in the NRGR formalism has been derived in [41]. However, when comparing our results one should be careful about the fact that [41] uses a different parametrization of the metric, namely the Kol-Smolkin (KS) variables [42], in which $h_{00} \sim e^{2\phi}$. Thus, our perturbation $h_{\mu\nu}$ contains in fact an infinite number of powers of ϕ . This means that our linearized Einstein-Hilbert action 5 contains an infinite number of bulk vertices in the KS variables (but not all of them). This makes a direct comparison with [41] difficult at the nonlinear level, so we rather chose to directly evaluate the Feynman diagrams without the KS variables.
- [33] A. Antonelli, A. Buonanno, J. Steinhoff, M. van de Meent, and J. Vines, Phys. Rev. **D99**, 104004 (2019), arXiv:1901.07102 [gr-qc].
- [34] Z. Bern, C. Cheung, R. Roiban, C.-H. Shen, M. P. Solon, and M. Zeng, Phys. Rev. Lett. **122**, 201603 (2019).
- [35] Z. Bern, C. Cheung, R. Roiban, C.-H. Shen, M. P. Solon, and M. Zeng, Journal of High Energy Physics **2019** (2019), 10.1007/jhep10(2019)206.
- [36] T. Damour, Physical Review D **94** (2016), 10.1103/physrevd.94.104015.
- [37] T. Damour, Physical Review D **97** (2018), 10.1103/physrevd.97.044038.
- [38] T. Damour, “Classical and quantum scattering in post-minkowskian gravity,” (2019), arXiv:1912.02139 [gr-qc].
- [39] A. Kuntz, In prep..
- [40] A. Buonanno and T. Damour, Phys.Rev.D **59**, 084006 (1999), arXiv:gr-qc/9811091.
- [41] J. B. Gilmore and A. Ross, Physical Review D **78** (2008), 10.1103/physrevd.78.124021.
- [42] B. Kol and M. Smolkin, Phys.Rev.D **77**, 064033 (2008), arXiv:0712.2822 [hep-th].